

**ANALYSIS OF HYDROTHERMAL SYNTHESIS OF $\text{SnO}_2 - \text{Al}_2\text{O}_3$
NANOCOMPOSITE**^{1a}Parveen Rathi, ²Manoj Kumar, ³Rajesh Sharma, ⁴Ritu¹ Research Scholar, ECE Deptt., Om Sterling Global University, Hisar, Haryana (India)² Associate professor, ECE Deptt., Om Sterling Global University, Hisar, Haryana (India)³ Assistant professor, Physics Deptt., MNS Govt. College, Bhiwani, Haryana (India)⁴ Assistant professor, Physics Deptt., Jagannath university, Bahadurgarh, Haryana (India)^aparveenrathivce@gmail.com

Abstract - There is a lot of interest in composites because their chemical and physical characteristics may be altered. Zinc acetate was used first; aluminum nitrate and sodium hydroxide were added later. X-ray powder diffraction (XRD) pattern of artificial Al_2O_3 showed that it had a hexagonal shape. $\text{SnO}_2 - \text{Al}_2\text{O}_3$ composites have garnered much interest due to their possible use in dye-sensitized solar cells and sensors. Composites of zinc oxide and aluminum oxide were synthesized using hydrothermal synthesis. The thermal characteristics of the nanopowder were determined using thermogravimetric analysis (TGA), and the optical and dielectric properties of the composite were determined using UV-V spectroscopy and dielectric analysis.

Keywords: SnO_2 , Al_2O_3 , Nanoparticles, Hydrothermal

Introduction

As a member of the II-VI oxide family, tin oxide (SnO_2) is a semiconductor with a wurtzite structure and a hexagonal crystalline arrangement of its atoms. Due to its large band gap ($E_g = 3.37$ eV) and high exciton binding energy, it may be used as a replacement for GaN in short-wavelength optoelectronic devices [1] (60 MeV). ZnO has been the subject of many studies because of its potential applications in various fields [2].

Ingestion of listeria monocytogenes (LMs) may result in serious illness or death [1-6]. This applies to the young, the old, and those with compromised immune systems. To keep track of LM infections without spending a tonne of money or effort on laborious and inefficient procedures such as detecting 3-hydroxy-2-butanone (3H-2B) markers (abundance: 20-30%) [7-9], gas detection equipment has become more popular.

Tin oxide (SnO_2) has been studied extensively to detect a select few target gases [12-14], but its potential for detecting the 3H-2B biomarker is little understood. There are a lot of factors, such as stability and selectivity, that contribute to a biomarker's credibility. Suppose you want to separate the 3H-2B biomarker from its reactive products and interfering gas. In that case, you'll require a sensing material with remarkable selectivity,

stability, ppb-level detection limit, and low operating temperature [15]. $\text{SnO}_2 - \text{Al}_2\text{O}_3$ core-shell nanorods [13] created as gas sensors may enhance selectivity and sensitivity by shielding the inner detecting materials from humidity and external chemicals. Tin oxide-based 3H-2B biomarker sensors with a discontinuous Al_2O_3 shell to shield them from the elements may have increased stability and sensitivity.

It is possible to create nanoparticles using various techniques, including hydrothermal, sol-gel, solvothermal, electrodeposition, and chemical vapor deposition. Hydrothermal is one of the easiest and cheapest techniques [16]. This study details the hydrothermal synthesis of $\text{SnO}_2 - \text{Al}_2\text{O}_3$ crystalline composites. We also detail how the reaction temperature and duration may affect the final $\text{SnO}_2 - \text{Al}_2\text{O}_3$ composite's performance metrics.

2. Experimental

Zinc acetate and aluminum nitrate were often blended in the right amounts with double-distilled water and agitated until the solutions became translucent, although this is not always the case. They were then swirled for 30 minutes to ensure proper mixing. Afterward [17], The solution was heated in an autoclave coated with Teflon for 2 hours at 180 degrees Celsius to 230 degrees Celsius (with a ramping temperature of 1 hour). Once the 15 hours at 80 degrees the temperature in the oven reached 100 degrees Celsius, the precipitates were washed many times in a mixture of double-distilled water and 100% ethanol to remove any remaining contaminants.

Field emission scanning electron microscope (FESEM), ultraviolet-visible spectrometry, and X-ray diffraction were used to characterize $\text{SnO}_2 - \text{Al}_2\text{O}_3$ composites synthesized hydrothermally. (UV), and X-ray diffraction (XRD). X-ray diffraction radiation $=1.5406\text{\AA}$ was used to determine the crystal structure [18]. SEM images were used to determine surface morphology (JEOL, JSM- 67001). Obtaining 200-1200 nm absorption spectra, a CARY 5E UV-VIS-NIR SPECTROPHOTOMETER was employed.

2.1 Synthesis of $\text{SnO}_2@ \text{Al}_2\text{O}_3$ NCBs

Figure 1 depicts the steps involved in creating $\text{SnO}_2@ \text{Al}_2\text{O}_3$ NCBs (a). The AAO forms were made the same way as in the published works. To be more specific, a graphite plate acts as the counter electrode, and a thin Au layer is sprayed onto each side of the AAO template to cover the pores completely. Before depositing Sn NWs, we blocked the nanopores in the base of the AAO template by depositing short-segmented Cu NWs in an electrolyte of 0.2 M CuSO_4 (pH = 4). Then, an electrolyte of 0.2 M SnSO_4 and 0.1M H_3BO_3 was subjected to a voltage constant of 1.5-2 V [19] for 120 minutes at room temperature (boric acid). Buffering with a diluted H_2SO_4 solution brought the electrolyte to a neutral pH of 3.4. Table 1 displays the percentages of $\text{SnO}_2@ \text{Al}_2\text{O}_3$ utilized in this paper.

Table 1 composition of $\text{SnO}_2 - \text{Al}_2\text{O}_3$ in nanocomposite

S. No.	SnO_2 (%)	Al_2O_3 (%)
1.	100	5

2.	100	10
3.	100	20
4.	100	0

2.2 Gas sensing Measurements

Our past research served as a blueprint for constructing sensor prototypes. A static testing facility was used to examine the gas detection capabilities of the device. $S = R_a/R_g$, where R_a and R_g determine the survivability of surrounding air and target gas, expresses the sensor's gas sensitivity. How long it takes for the sensor's resistance to return to 90% of its original value after an adsorption or desorption event is known as the reaction time or recovery time, respectively.

2.3. $\text{SnO}_2@/\text{Al}_2\text{O}_3$ nanocomposites Synthesis

Synthesis of SnO_2/C composites used a method that deviates somewhat from pure carbon due to incorporating 0.04 g of aluminum oxide Al_2O_3 NCs. The steps required to produce $\text{SnO}_2@/\text{Al}_2\text{O}_3$ NCs are as follows: The samples were obtained after 5 hours of continuous grinding. For 15 hours, powdered SnO_2 NPs (as-prepared) were mechanically processed in a high-energy ball mill alongside aluminum oxide nanocrystals, Al_2O_3 NCs (0.04 g). After determining the alumina percentage, 0.074 grams of graphite nanosheets were added to the mixture.

3. Results and discussion

Hydrothermally produced products (180°C - 230°C) were subjected to an XRD pattern analysis (Figure 1). In X-ray powder diffraction analysis, the product displays peaks consistent with a hexagonal structure and a lattice constant of $a = 3.239$ and $c = 5.176$. Tile no. 89-7162 in the JCPDS According to Scherer's formula applied to X-ray diffraction data, the typical grain size is 32.9 nm.

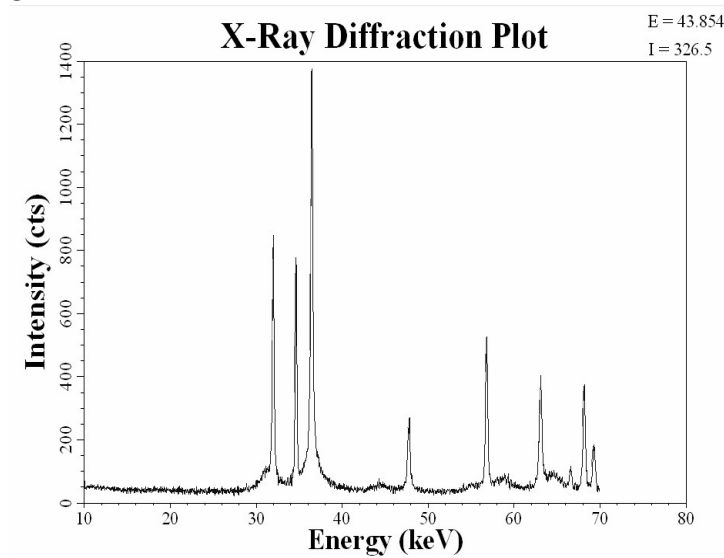


Figure 1: XRD analysis of $\text{SnO}_2\text{-Al}_2\text{O}_3$ composites

UV analysis of $\text{SnO}_2 - \text{Al}_2\text{O}_3$ composites annealed at 80°C for 15 hours is shown in Figure 2. At 371.87 nm , we find the absorption peak. The resultant band gap energy was determined to be 3.347 eV .

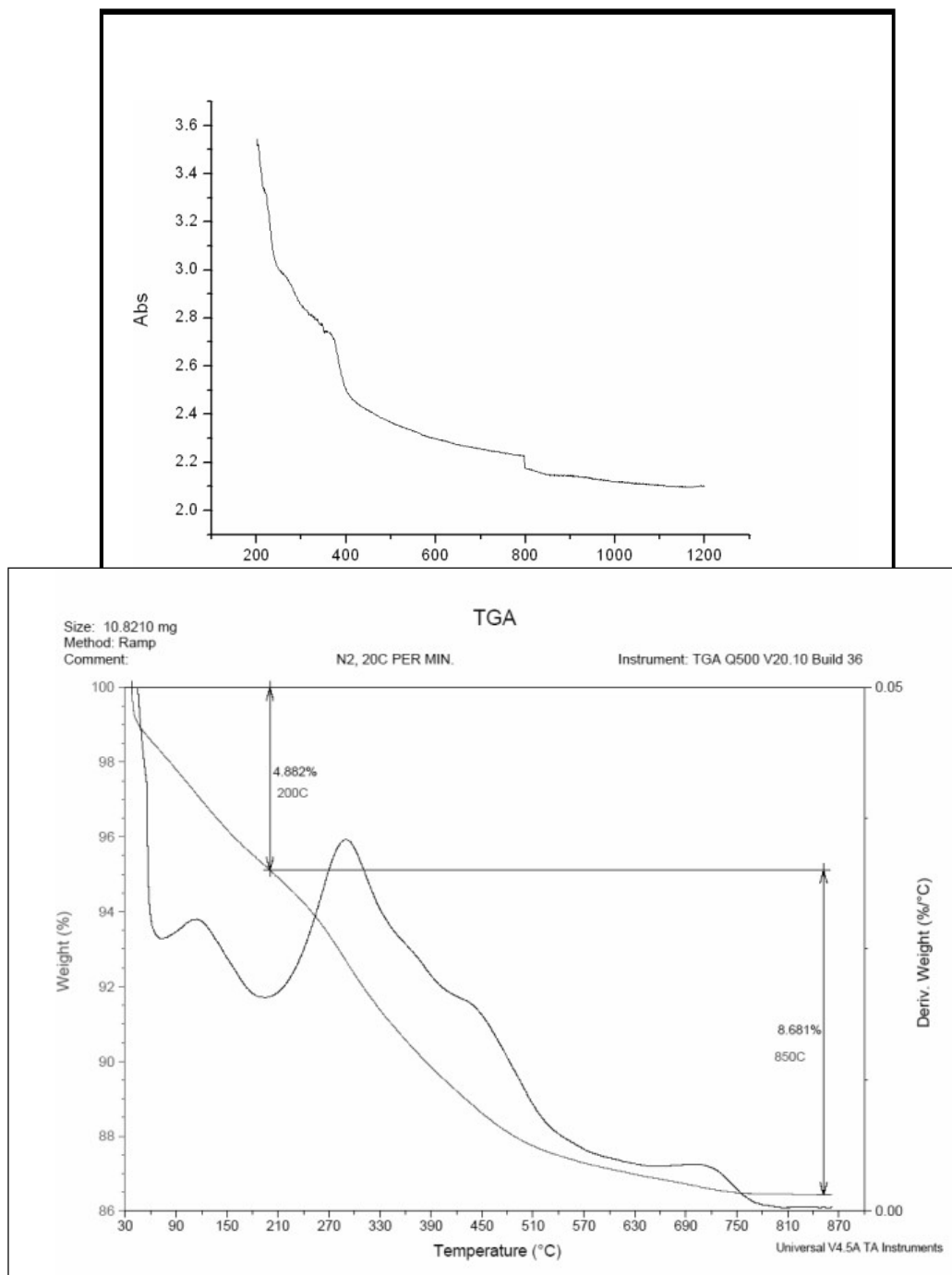


Figure 3: Thermal Analysis of the $\text{SnO}_2 - \text{Al}_2\text{O}_3$ composite

The results of a thermal analysis performed on composites with zinc oxide and aluminum oxide are shown in Figure 3. Aluminum and zinc oxide nanoparticles were heated from ambient temperature to 900 degrees Celsius in a stream of Nitrogen. According to the TGA curve, the precursor loses 4.88 percent of its mass between 30

and 200 degrees Celsius and another 8.681 percent at 850 degrees Celsius. There was an initial drop in mass due to the loss of interlayer and water content via evaporation. Around 330 degrees Celsius, nucleation and combustion of organic molecules reach a climax. The graph shows that at higher temperatures, mass loss occurs more quickly. The surface morphology of $\text{SnO}_2 - \text{Al}_2\text{O}_3$ composite sample particles has been studied using a field emission scanning electron microscope. Figure 4 shows FESEM and EDAX pictures of a sample of $\text{SnO}_2 - \text{Al}_2\text{O}_3$. Higher resolution FESEM imaging of the mixed sample revealed rod-like structures of around 200 nm in length and 40 nm in breadth and tiny particle-like structures of approximately 30 nm in size.

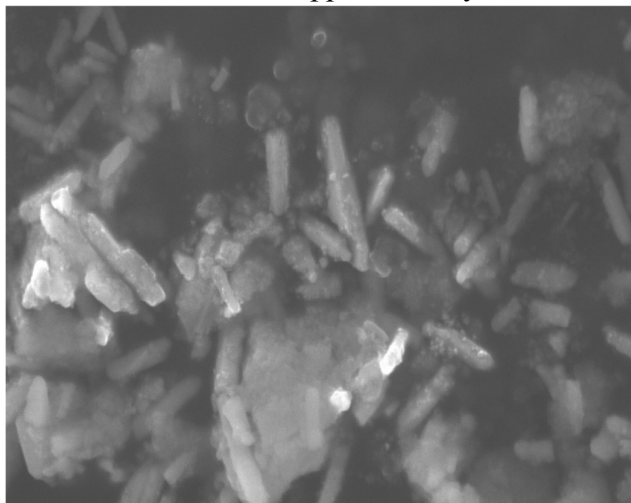


Figure 4: FE-SEM images of as-synthesized $\text{SnO}_2 - \text{Al}_2\text{O}_3$ nanoparticles

Figure 5 displays the dielectric constant curve vs. the application frequency. The dielectric constant is found to be highest in the low-frequency zone and to decrease with increasing frequency. Space charge, orientation, electronic, and ionic polarization may contribute to the large value of (ϵ') at low frequencies. At the same time, their relative insignificance may account for the smaller values at higher frequencies. This was seen in composite samples of $\text{SnO}_2 - \text{Al}_2\text{O}_3$.

5. Conclusion

Aluminum oxide (alumina) is the material of choice for many applications due to its outstanding dielectric characteristics and thermal properties, while tin oxide (SnO_2) is a well-studied broad-band semiconductor. $\text{SnO}_2 - \text{Al}_2\text{O}_3$ combination has become one of the most promising transparent conductive oxides in recent years. The band gap was computed using excitonic peaks of the UV absorption curve and agreed with a direct band gap of corresponding substances.

SnO_2 nucleation has been seen to occur at 338.1°C , a metastable state has been formed in aluminum oxide, and a proportion of sample weight has been lost due to heating. Characteristics of the sample's surface were obtained using FESEM. The relevance of the samples' dielectric qualities may be better grasped after conducting dielectric research.

References

1. Biswas S and Kar S J. *Appl. Phys. Nanotechnology* 045710, 2008, 19
2. Wei Lan, Xingping Peng, Xueqin Liu, Zhiwei He and Yinyue Wang, Preparation and properties of ZnO thin films deposited by sol-gel technique, *Front. Mater. Sci. China* 1(1): 2007, 88–91
3. Thanh Binh Nguyen, Thi Thanh Binh Le, Ngoc Long Nguyen, The preparation of SnO_2 and SnO_2 : Sb nanopowders by a hydrothermal method, *Adv. Nat. Sci.: Nanosci Nanotechnol.* 025002, (2010), 1
4. Hu J Q, Bando Y and Golberg D, Self-catalyst growth and optical properties of novel SnO_2 fishbone-like nanoribbons, *Chem. Phys Lett.* 372, 2003, 758-762
5. J. Q. Hu, X. L. Ma, N. G. Shang, et al., Large-Scale Rapid Oxidation Synthesis of SnO_2 Nanoribbons, *Journal of Physical Chemistry B*, vol. 106, 15, 2002. , 3823– 3826,
6. Gu F, Wang S F, Lü M K, Zhou G J, Xu D, and Yuan D R, Photoluminescence Properties of SnO_2 Nanoparticles Synthesized by Sol–Gel Method, *J. Phys. Chem. B* 108, 2004, 8119
7. E. R. Leite, I. T. Weber, E. Longo, and J. A. Varela, A New Method to Control Particle Size and Size Distribution of SnO_2 Nanoparticles for Gas Sensor Applications, *Advanced Materials*, vol. 12, no. 13, 2000, 965–968,
8. G. S. Pang, S. G. Chen, Y. Koltypin, A. Zaban, S. Feng, and A. Gedanken, Controlling the Particle Size of Calcined SnO_2 Nanocrystals, *Nano Letters*, vol. 1, no. 12, 2001, 723–726,
9. Zhu H, Yang D, Yu G, Zhang H, and Yao K, A simple hydrothermal route for synthesizing SnO_2 quantum dots, *Nanotechnology* 17, 2006, 2386–2387
10. Xu J, Yang H, Yu Q, Chang L, Pang X, Li X, Zhu H, Li M and Zou, Synthesis and characterization of hollow glass microspheres coated by SnO_2 nanoparticles, *Mater. Lett.* 61 G, 2007, 1424
11. Zhang J and Gao L, Synthesis and characterization of antimony-doped tin oxide (ATO) nanoparticles by a new hydrothermal method, *Mater. Chem. Phys.* 87, 2004, 10
12. Miao H, Ding C, and Luo H, Antimony-doped tin dioxide nanometer powders prepared by the hydrothermal method, *Microelectron. Eng.* 66, 2003, 142
13. Li C and Hua B, Preparation of nanocrystalline SnO_2 thin film coated Al_2O_3 ultrafine particles by fluidized chemical vapor deposition, *Thin Solid Films* 310, 1997, 238

14. Jeong J, Choi S P, Chang C I, Shin DC, Park J S, Lee B T, Park Y J and Song H J, Photoluminescence properties of SnO_2 thin films grown by thermal CVD, *Solid State Commun.* 127, 2003, 595
15. Moulson, A. J.; Herbert, J. M., *Electroceramics: Materials, Properties, Applications*, Electroceramics, Chapman & Hall, New York, 1990
16. Y. Shimizu, M. Egashira, Basic aspects and challenges of semiconductor gas sensors, *MRS Bull.*, 24, 1999, 18-22.
17. Wang, H. C.; Li, Y.; Yang, M. J., Fast response thin-film SnO_2 gas sensors operating at room temperature, *Sens. Actuators. B Chem.* 119, 2006, 380-383.
18. Li, G. J.; Zhang, X. H.; Kawi, S., Relationships between sensitivity, catalytic activity, and surface areas of SnO_2 gas sensors, *Sens. Actuators. B Chem.*, 60, 1999, 64-70.
19. Muhammad Akhyar FARRUKH, Boon-Teck HENG, Rohana ADNAN, Surfactant-controlled aqueous synthesis of SnO_2 nanoparticles via the hydrothermal and conventional heating methods, *Turk J Chem* 34 (2010), 537 – 550.